Bioactive Diterpenoids Impact the Composition of the Root-Associated Microbiome in Maize (Zea mays)

Katherine M. Murphy
University of California Davis
Joseph Ewards
University of Texas at Austin
Katherine B. Louie
E O Lawrence Berkeley National Laboratory
Benjamin P. Bowen
E O Lawrence Berkeley National Laboratory
Venkatesan Sundaresan
University of California Davis
Trent R. Northen
E O Lawrence Berkeley National Laboratory
Philipp Zerbe (pzerbe@ucdavis.edu)
University of California Davis https://orcid.org/0000-0001-5163-9523

Research

Keywords: Maize, rhizosphere, microbiome, diterpenoids, terpene metabolism, plant-environment interactions

Posted Date: April 14th, 2020

DOI: https://doi.org/10.21203/rs.3.rs-21333/v1

Version of Record: A version of this preprint was published at Scientific Reports on January 11th, 2021.
See the published version at https://doi.org/10.1038/s41598-020-79320-z.

Abstract

Background : Plants deploy both primary and species-specific, specialized metabolites to communicate with other organisms and adapt to environmental challenges. This includes interactions with soil-dwelling microbial communities, where plants may exchange sugars for important nutrients and protection against environmental perturbations, directly benefitting plant fitness. However, the molecular mechanisms underlying these plant-microbe interactions often remain elusive.

Results : In this study, we report that maize (Zea mays) specialized diterpenoid metabolites with known antifungal bioactivities also influence rhizosphere bacterial communities. Metabolite profiling showed that dolabralexins, antibiotic diterpenoids that are highly abundant in roots of some maize varieties, can be exuded from the roots. Comparative 16S rRNA gene sequencing determined the bacterial community composition of the maize mutant Zman2 (anther ear 2), which is deficient in dolabralexins and closely related bioactive kauralexin diterpenoids. Under well-watered conditions, the Zman2 rhizosphere microbiome differed significantly from the wild-type sibling with the most significant changes observed for Alphaproteobacteria of the order Sphingomonadales. By contrast, there was no difference in the microbiome composition between the mutant and wild-type was observed under drought stress. Metabolomics analyses support that these differences are attributed to the diterpenoid deficiency of the Zman2 mutant, rather than other metabolome alterations.

Conclusions : Together, these findings support physiological functions of maize diterpenoids beyond known chemical defenses, including the assembly of the rhizosphere microbiome.

Background

Extensive research in recent years has demonstrated the composition and importance of rhizosphere microbial communities to plant health and fitness [1–3]. The cooperative partnership of microbes and plants has been attributed largely to an exudation of photosynthate sugars from the plant in exchange for nutrient supply and protection against biotic and abiotic stress, ultimately contributing to increased plant vigor and yield [4, 5]. Despite extensive characterization of species- and tissue-specific microbial communities and how these vary in their ecological and genetic contexts, our understanding of the mechanisms by which plants recruit and maintain root-associated microbial communities is still limited [5–11].

As the most economically important crop in the United States, maize (*Zea mays*) has been the subject of long-standing research to improve crop yield and stress resilience traits [12]. The “core” microbiome of maize has provided insights into the presence of specific phyla in and near maize roots [6, 13, 14]. A study of 27 maize inbred lines across developmental stages and geographical locations demonstrated maize genotype as a replicable factor in defining the microbiome, with significant variation due to the different genetic backgrounds among inbred lines. Five “core” Operational Taxonomic Units (OTUs), all in the phyla Proteobacteria, were found to be present in all samples [14]. Drawing on these detailed insights

into the maize microbiome, further research has ventured into determining the chemical signaling factors that determine microbiome composition and variation across genotypes. Specialized metabolites mediate various plant interactions with the environment and other organisms, and several major bioactive metabolite groups have been identified in maize, including diterpenoids, sesquiterpenoids, oxylipins, and benzoxazinoids [15–20]. Given their distinct structures, bioactivities and abundance across different maize tissues and developmental stages, maize specialized metabolites can be hypothesized to play a critical role in the plant communication with root-borne microbes and thus help determine the root microbiome. Recently, benzoxazinoids were shown to influence the maize response to stress via altered rhizosphere microbial communities mediated by 6-methoxy-benzoxazolin-2-one (MBOA) [21]. Additional work on benzoxazinoids mutants showed changes to fungal and bacterial communities as a result of benzoxazinoid deficiency [22]. Furthermore, benzoxazinoid-deficient mutants were shown to feature dramatically altered root metabolomes, suggesting alterations in the microbiome may not be solely attributed to a lack of specific benzoxazinoids, but rather global changes in root metabolites in mutant plants [23]. Alongside these findings, there is a large degree of variation in the observed differences in alpha and beta diversity in benzoxazinoid mutants [21–23].

The diverse group of terpenoid metabolites also has shown to be critical in mediating above- and below-ground interactions between plants and other organisms, including microbes [24]. Kauralexins and dolabralexins are two major diterpenoid groups in maize that have demonstrated or predicted roles in biotic and abiotic stress responses [16–18, 25]. Kauralexins show stress-elicited accumulation in several tissues, including stems and scutellum, and mediate quantitative defenses against fungal pathogens such as species of *Fusarium*, *Aspergillus* and *Cochliobolus*, as well as insect pests including the European corn borer (*Ostrinia nubilalis*) [17, 26–28]. The more recently discovered group of dolabralexins shows pathogen-inducible accumulation predominantly in roots and, like kauralexins, have strong growth-inhibitory activity against *Fusarium* pathogens [18]. In addition to their defensive potential against biotic stressors, both kauralexin and dolabralexin production was shown to be increased in response to abiotic stress, such as drought or oxidative stress [16, 18]. Kauralexins and dolabralexins derive from a common precursor, *ent*-copalyl diphosphate (*ent*-CDP), which is also shared with the gibberellin (GA) biosynthetic pathway critical for plant growth (Fig. 1) [17, 29]. Two catalytically redundant diterpene synthase (diTPS) enzymes, ANTHER EAR 1 (ZmAn1) and ANTHER EAR 2 (ZmAn2) control *ent*-CDP formation in maize [29, 30]. Genetic studies revealed that *ZmAn1* is critical for GA biosynthesis, whereas ZmAn2 feeds *ent*-CDP into kauralexin and dolabralexin biosynthesis, thus enabling a pathway partition separating precursor flux toward general and specialized diterpenoid pathways [29–31] (Fig. 1). This pathway separation is supported by the phenotype of the *Zman2* mutant, which features a loss of function in the *Zman2* gene through a stable Ds insertion from the Activator (Ac) and Dissociation (Ds) system [16, 29]. *Zman2* has kauralexin and dolabralexin deficiency but normal GA levels [16]. Although it has a normal growth phenotype, *Zman2* shows increased susceptibility to biotic and abiotic stress as compared to its WT sibling, consistent with the protective bioactivity of kauralexins and dolabralexins [16]. This phenotype, paired with the bioactivity of maize diterpenoids and their accumulation in roots in

response to abiotic stress, suggests a possible role of these metabolites in broader plant-microbe interactions, including root microbiota.

To test this hypothesis, we investigated the microbial communities of the diterpenoid-deficient *Zman2* mutant compared to its wild type (WT) sibling under both well-watered and drought conditions. Using sequencing of the microbial 16S rRNA gene, we detected and classified OTUs to analyze the structure and variation of bacterial communities in both the rhizosphere and endosphere. We subsequently provide evidence that dolabralexins can be exuded from the roots, and that the *Zman2* mutant lacks other significant metabolic changes other than diterpenoid content, suggesting that diterpenoid deficiency is responsible for the altered microbiome.

Results

Dolabralexins are secreted outside of maize roots

To examine a possible role of maize diterpenoids in plant-microbiome interactions, we utilized the *Zman2* mutant genotype in comparison to its isogenic WT sibling [16, 29]. Previous studies showed that 30-day-old WT maize plants significantly accumulate dolabralexins, and to a lesser extent kauralexins, in roots [16], whereas the *Zman2* mutant genotype is almost completely devoid of these diterpenoids [16–18]. Despite the deficiency of both kauralexins and dolabralexins in *Zman2* root tissue, mutant plants did not show an apparent phenotype under well-watered conditions (Fig. 2A), consistent with prior reports describing largely unaltered root and shoot weight, developmental features, and GA and zealexin levels in the *Zman2* mutant [16]. *Zman2* plants were used as a control for analyzing root metabolite exudation due to the deficiency of diterpenoids, and subsequent analysis of the microbiome and metabolome.

To determine a possible ability of maize diterpenoids to affect the rhizosphere microbiome, we first tested if diterpenoids can be exuded from maize roots. For this purpose, 38-day-old maize plants, both *Zman2* and its WT sibling, were grown on soil then gently cleaned and subsequently suspended for 48 hours in nutrient water. After removing the plants, metabolites were extracted from the nutrient water using an equal volume of ethyl acetate and analyzed by LC-MS/MS against authentic metabolite standards. As a positive control, the benzoxazinoid 1,3-benzoxazol-2-one (BOA), known to be secreted from maize roots, was measured and used as a standard to detect BOA and other benzoxazinoids metabolites with similar mass spectra. Benzoxazinoids were found to be present in both *Zman2* and WT plant exudates, while absent in nutrient water without plants, as expected (Fig. 2B). Of the known dolabralexins for which standards were available – epoxydolabradiene, epoxydolabranol, and trihydroxydolabrene – only trace amounts were detected in nutrient water after incubation of the *Zman2* mutant (Fig. 2B), as expected based on the known mutant phenotype. Trihydroxydolabrene and epoxydolabradiene were both significantly enriched in the WT root exudate samples than *Zman2* or nutrient water without plants (Fig. 2B). Epoxydolabranol was not detected in mutant nor WT plant exudates.

Maize Root Microbial Communities Are Distinct By Compartment

The *Zman2* mutant genotype and its corresponding WT sibling serve as a tool to investigate the effect of diterpenoids, or the lack thereof, on the maize root microbial community [16, 18]. Under abiotic stress conditions, while WT maize plants were shown to have increased levels of kauralexin and dolabralexin metabolites and a greater root/shoot ratio, *Zman2* plants were shown to be more susceptible to stress conditions via earlier onset of leaf curling and a reduced root/shoot weight ratio [16]. Based on this knowledge and the growth conditions of previous research on the mutant genotype, we used one-month-old *Zman2* and isogenic WT sibling plants to comparatively examine the impact of diterpenoid-deficiency on the maize root microbiome. Half of the plants were treated with drought stress in order to investigate if changes in the microbiome exist under ideal and/or stress conditions, and if these changes may suggest an influence on the *Zman2* ability to cope with abiotic stress. Representative plant images are shown in Fig. 2A.

Microbiomes of the rhizosphere (1–2 mm of soil outside the root) and endosphere (inside the root), the latter representing root samples after removal of rhizosphere and rhizoplane microbes through washing and sonication of the roots, were analyzed. Bulk soil without plants was used as a control to examine background soil microbial communities. The 16S rRNA gene (V4 region) was sequenced using Illumina MiSeq and sequences were clustered into operational taxonomic units (OTUs) using the QIIME pipeline and the Greengenes database [32]. After filtering to remove mitochondrial and chloroplast OTUs, 4,259 distinct OTUs remained. OTU counts were then normalized by relative abundance, which was used rather than rarefaction methods so as not to discard low abundance OTUs. In all, four factors were analyzed: compartment, genotype, water status, and the interaction between genotype and water status.

Consistent with previous research in maize and other plant species [7, 33], the microbial communities of the two plant compartments and the bulk soil were all statistically distinct. The alpha diversity, as measured by the Shannon index, showed the greatest diversity of microbes in bulk soil, with reduced diversity in the rhizosphere and further reduction in the endosphere (Fig. 3). A permutational multivariate analysis of variance (PERMANOVA) was used to measure the diversity between samples (beta diversity) and showed that, when accounting for all factors, compartment accounts for 23% of the variation between samples ($p < 0.001$). This was confirmed by a principle coordinate analysis (PCoA), in which compartment was the greatest source of variation (Fig. 4). A total of 960 OTUs, in 21 phyla (out of 32 total phyla), were enriched in the rhizosphere as compared to the endosphere, whereas 82 OTUs in 9 phyla were enriched in the endosphere as compared to the rhizosphere, as determined using the DESeq2 package in R. Among the 10 most abundant phyla plotted for each sample type, some phyla were found to be enriched in both compartments, whereas the rhizosphere was predominantly enriched for OTUs in the phyla Actinobacteria, Acidobacteria, and Alphaproteobacteria (Fig. 5).

The endosphere did not demonstrate significant differences attributed to genotype, water treatment, nor their interaction, as determined by PERMANOVA and PCoA (Fig. 4B). No individual OTUs were

significantly enriched or depleted in regards to sample type in the endosphere as analyzed by generalized linear models. Because there was no apparent difference, all further analysis focuses on the rhizosphere compartment only, and the bulk soil and endosphere samples were omitted from further analyses.

Rhizosphere Microbial Communities Are Distinct Under Different Watering Conditions

Drought was defined in this study as a withholding of water for seven days, with a single watering on day four. For both WT and *Zman2*, drought-treated plants showed severe leaf curling, but were still green and not wilted over completely (Fig. 2A). Volumetric water content (VWC) of the soil surrounding well-watered plants was 10.7 ± 1.9 percent, while drought plants was 6.9 ± 1.9 percent. When accounting for all rhizosphere samples, water status accounted for 12.6% of the observed microbiome variation ($p < 0.001$), and visibly separated sample types in a principal components analysis (Fig. 4C).

We next identified OTUs enriched or depleted across treatments using the R software package DESeq2. When including all plants, irrespective of genotype, drought-stressed plants were enriched for 51 OTUs, which were predominantly composed of taxa from the Phylum Actinobacteria (Fig. 6A, OTU abundances by sample type in Supplemental Fig. 1). Well-watered plants were enriched for 97 OTUs as compared to drought conditions, mostly represented by Bacteriodetes, Alphaproteobacteria, Gammaproteobacteria, and Betaproteobacteria (Fig. 6A, OTU abundances by sample type in Supplemental Fig. 2). In bulk soil samples, 21 OTUs, including Bacteroidetes and Verrucomicrobia, were enriched, whereas six OTUs, primarily Actinobacteria, were depleted under well-watered conditions (Fig. 6B). Of these, 21 significant OTUs were also enriched or depleted in the rhizosphere samples as compared to the bulk soil control samples, suggesting they are influenced by drought stress regardless of any plant-microbe interactions (Fig. 6C). Together, these results are consistent with the demonstrated contribution of water status to the rhizosphere microbiome composition [33–35], and suggest that environmental as well as host-controlled processes influence the composition of rhizosphere-associated microbiomes under drought stress.

The Zman2 mutant features a distinct microbial community composition

Next, the impact of genotype on the rhizosphere microbiome composition was assessed by investigating each water status separately for genotype effects by water treatment (GxD). Under well-watered conditions, significant differences in the microbiome composition were observed between WT and *Zman2* plants, with genotype accounting for 5.8% of the variation for well-watered samples alone ($p < 0.05$). *Zman2* plants harbor a more diverse microbiome as determined by a greater alpha diversity compared to the WT sibling (Fig. 3). Six OTUs were more abundant in WT plants, whereas none were enriched in *Zman2* samples (Fig. 7; OTU abundances by sample type plotted in Supplemental Fig. 3). Of the six OTUs, all were assigned to Alphaproteobacteria belonging to the order Sphingomonadales, three

of which were assigned to the genus Sphingobium, whereas the remaining OTUs were unclassified at the genus level.

In contrast to well-watered conditions, there is much less variation in the rhizosphere microbiome of WT and *Zman2* under drought conditions. Distance-based approaches analyzing beta diversity, analyzing variance between samples, showed them to be indistinguishable. In addition, no differences in the alpha diversity (variance within a sample) were observed between the two genotypes under drought conditions. However, a handful of individual OTUs are significantly differentially abundant between the two genotypes when determining individual OTUs that were significantly different: six were enriched in *Zman2* (including Sphingomonadales and Enterobacteriales) and none were significantly enriched in WT (Fig. 7; Supplemental Fig. 3).

Genotype By Environment Interaction Suggested By Microbial Communities

A genotype by environment (GxE) interaction is implied by the different responses of the *Zman2* and WT genotypes to drought stress. This is reflected by the interaction of genotype:water status, which accounts for 5.3% of the variation in beta diversity in all rhizosphere samples ($p < 0.05$) and by the principal component analysis, in which *Zman2* and WT are separate under well-watered conditions, but converge to have the same beta diversity under drought conditions (Fig. 4C). Analysis of the GxE interaction using log ratio tests of full and reduced models in DESeq2 determined that one Chitinophagaceae and one Sphingomonadales OTU were significantly impacted by this interaction (OTU abundances plotted by sample type in Supplemental Fig. 4).

Since the microbiome compositions between *Zman2* and WT genotypes differed much more under well-watered but not drought conditions, we analyzed both water statuses separately for each genotype to look at drought effects on each genotype (DxG). This analysis revealed that drought had a larger effect on WT, in which 70 OTU were enriched and seven were depleted under well-watered conditions as compared to drought stress, and drought-exposed plants had a greater alpha diversity. In comparison, for *Zman2*, only 12 OTU were enriched and six depleted in well-watered conditions, and drought treatment did not impact the alpha diversity.

Dolabralexins, but not other specialized metabolites, are more abundant in wild type plants

To verify that differences in microbiome composition can be attributed to a deficiency in diterpenoids in the roots of *Zman2* plants, metabolite profiling using both targeted and untargeted LC-MS/MS analysis was performed on the same root samples used for microbial composition analysis. Targeted metabolite analysis of the major dolabralexin metabolite, trihydroxydolabrene (THD) confirmed via a standard that THD was near absent in the *Zman2* mutant while present in WT under well-watered conditions (Fig. 8).

Epoxydolabranol was not found in either mutant nor WT plants (Supplemental Fig. 5), while epoxydolabradiene was found to be lowly abundant in both mutant and WT plants (Fig. 8), presumably because of their conversion to THD. Dolabralexins were not significantly enriched in WT versus *Zman2* under drought conditions, due to notable variation between individual WT plants, but were still markedly trace in *Zman2* drought plants (Fig. 8). Mirror plots demonstrate these identifications, as well as their absence in the mutant plants (Supplemental Fig. 5). This observation is consistent with previous research, showing low levels of dolabralexin and kauralexin metabolites in *Zman2*, predictably due to *ent*-CDP derived from ZmAn1 activity [16]. As a control, benzoxazinoid abundance was calculated using BOA as a standard, and found to be present in both *Zman2* and WT roots without significant differences in abundance between well-watered and drought-stressed plants. Using BOA for LC-MS/MS generates multiple peaks with similar mass spectra due to various benzoxazinoids compounds, and their total area was analyzed here (Supplemental Fig. 5).

Parallel untargeted metabolomics analysis also did not indicate any significant variance in the metabolite profiles of the WT and *Zman2* plants beyond the focal diterpenoids (Fig. 9A and B). Two observed data points of significant difference represented the same plants in both positive and negative mode (Fig. 9A and B). PERMANOVA analysis based on all dominant mass ions and corresponding specific retention times demonstrated neither genotype nor water status significantly impacted the metabolome using either positive or negative ionization modes. This result was further corroborated by a PCoA (Fig. 9A and B). Although the PERMANOVA and PCoA demonstrated no significant difference overall between sample types, a generalized linear model was used to identify individual metabolites that may be significantly enriched or depleted. A total of 111 metabolites were enriched in WT as compared to 85 enriched in *Zman2* under well-watered conditions using positive ionization mode (Fig. 9C, Supplemental Table 1). Consistent with the targeted metabolite profiling, THD was among the 111 enriched metabolites in WT roots. Annotation of the remaining metabolites with distinct profiles in WT and *Zman2* roots by comparison to mass spectral databases identified significant matches for 53 compounds, representing 27% of the differentially abundant metabolites (Supplemental Table 1). Further metabolite annotation using the PACTOLUS method generated significant matches for an additional 113 compounds (Supplemental Table 1). Although a few metabolites were enriched or depleted in abundance between WT and *Zman2* plants (Fig. 9C, Supplemental Table 1), no other alterations in the metabolite profile were identified as significant, and the distinct abundance of dolabralexins was the dominant change in the overall metabolome composition of *Zman2* and WT roots. The analysis was repeated for differences between the genotypes under drought conditions (in which the microbiomes are more similar), and less metabolites were significantly different (Fig. 9C, Supplemental Table 2).

Similar to genotype, drought stress did not significantly affect the metabolite profiles of the WT or *Zman2* roots (Fig. 9A and B), as determined by PERMANOVA and PCoA. While the metabolite compositions variance between genotypes was not greater than the variance within the genotypes, there was a handful of metabolites that were determined to be significantly enriched or depleted, as determined by linear models. There was a significant enrichment of 99 metabolites in WT plants and 283 metabolites in *Zman2* plants under drought stress as compared to well-watered plants (Fig. 9C, Supplemental Tables 3

and 4). By comparison, 36 and 88 metabolites were enriched under well-watered conditions in WT and *Zman2* roots, respectively, as compared to drought (Fig. 9C, Supplemental Tables 3 and 4). While there are limited numbers of metabolites that change their abundance between drought and well-watered conditions, the overall metabolomes and variance between watering statuses remains statistically indistinguishable by PERMANOVA and PCoA.

Discussion

The dynamic interrelations between plants and their species-specific root microbiota directly influence plant health and stress tolerance [4]. Despite the importance of these mutualistic relationships, the underlying chemical mechanisms coordinating inter-organismal interactions remain largely elusive. In particular, limited knowledge exists on how specific metabolites, blends thereof, and the corresponding pathways impact plant-microbe interactions and microbial community assembly. For example, recent maize studies illustrated that mutant genotypes deficient in benzoxazinoid metabolites (specifically MBOA) showed an altered stress response mediated by the influence of MBOA on the below-ground microbial community, thus underscoring the importance of these metabolite-guided plant-microbe interactions on plant health [21–23]. In this study, we show that specific groups of bioactive diterpenoids in maize, namely dolabralexins and/or kauralexins, also contribute to the assembly of the rhizosphere microbiome.

Although the underlying secretion mechanisms require further study, presence of dolabralexins in maize root exudates supports a possible role of these compounds in below-ground plant-microbe interactions (Fig. 2). Microbiome analysis of the root microbial communities showed no significant influence of genotype or water status on endosphere communities using distance-based methods (Fig. 4). This observation differs from prior maize studies, which showed variation in the endosphere communities under well-watered or drought conditions [33]. Considering the diversity and dynamics of plant root microbiomes and metabolite blends, these contrasting findings may be attributed to differences in plant age, soil, and extent of droughting [36]. It appears plausible that diterpenoids do not impact endophytic microbes due to the spatial separation of endophytic microbes that predominantly colonize the apoplast [37, 38], whereas functionalized diterpenoids accumulate intracellularly as demonstrated in several plant species [39–41]. Substantiating previous research on root microbiomes in maize, the maize rhizosphere microbiome was significantly different between well-watered and drought stress conditions, regardless of genotype (DxG) (Fig. 4) [33, 34]. Phyla known to be influential in the plant response to drought, including Actinobacteria, were found enriched under drought conditions (Fig. 6) [33, 35]. Our results showing distinct rhizosphere microbial communities of *Zman2* and its WT sibling under well-watered conditions with a more diverse root microbiome alpha diversity in *Zman2* (Fig. 3), provide evidence supporting a role of diterpenoids in the microbiome assembly by reducing the community diversity. This is further supported by the distinct beta diversity between *Zman2* and WT under well-watered conditions (Fig. 4), with genotype accounting for 11% of the variation between samples. Notably, the significant differences between the two genotypes were defined by only a few OTUs, most of which were assigned to the order Sphingomonadales (Fig. 7). Sphingomonads have been reported to degrade phenolic compounds and

utilize them as carbon sources [42], and were among the OTUs displaying the greatest heritable variation (H^2) across maize lines of the NAM (Nested Association Mapping) diversity panel [14]. Considering the variation of dolabralexins across selected maize inbred lines [18], it can be speculated that not only phenolics, but also maize-specific diterpenoids mediate the interaction with species of Sphingomonadales.

The overall increased microbiome diversity in the *Zman2* mutant stands in contrast to previous research supporting that a greater microbial diversity promotes crop resistance to soil pathogens (Fig. 3) [43, 44], given that previous work has shown *Zman2* to be more susceptible to fungal pathogens [29]. Considering these findings in association with the demonstrated anti-microbial activity of both kauralexins and dolabralexins [17, 18], the relationship between the disease-preventative properties of dolabralexins and bacterial diversity remains more complex, and microbe-microbe interactions likely play an important role determining the overall microbial diversity phenotype.

Despite distinct alpha and beta diversities under well-watered conditions, the *Zman2* and WT communities were not distinguishable in their diversity or composition under drought stress using distance-based approaches (Fig. 3). While the drought-stressed communities of WT and *Zman2* were indistinguishable, their response to drought in terms of the changes in enrichment and depletion associated with differences with their respective well-watered samples was different. This is substantiated by the significant factor of the interaction between genotype and water status, a GxE interaction. While WT experienced significant changes in relative abundance of OTUs between well-watered and drought conditions, *Zman2* had fewer OTUs altered and no significant change in alpha diversity (Fig. 3), supporting the observation that *Zman2* plants have a lower capacity for environmental adaptation [16, 45]. The protective properties of kauralexins and dolabralexins have been previously described, in which *Zman2* is more susceptible to drought stress [16]. This protective mechanism may be hypothesized to be a result of interactions with rhizosphere microbes, in which these diterpenoids contribute to a specific community being selected for in the WT plant under well-watered conditions. This, in turn, may subsequently provide enhanced resilience under environmental stress conditions.

However, under continued drought stress, other factors than diterpenoid bioactivity seemingly become pertinent in the assembly of the rhizosphere microbiome, leading to a convergence of the WT and *Zman2* communities to become indistinguishable (Fig. 4). This is consistent with the fact that the levels of dolabralexins in WT plants remained largely unaltered in response to drought stress (Fig. 8). By contrast, earlier research showed drought-induced accumulation of kauralexins [16]. This discrepancy in inducible diterpenoid formation may result from differences in the selected maize genotype or plant cultivation and drought treatment conditions, considering the large variation of diterpenoid metabolism across maize genotypes and environmental stimuli [17, 18].

Recent research into the effect of benzoxazinoids provides insight into the magnitude of these changes and their importance to plant health. For example, decreased MBOA abundance in a defined benzoxazinoid maize mutant affected the plant stress response via the influence of MBOA on the below-

ground microbial community [21]. Unlike maize diterpenoids, which significantly changed alpha and beta diversity in the present study (Fig. 3), benzoxazinoids did not affect either the diversity or composition of microbial communities using distance-based approaches, with the exception of MBOA shown to affect select OTUs with a resulting impact on plant fitness [21, 46]. However, recent studies investigating the same genes targeted for mutation (*Zmbx1*, *bx2*, and *bx6*) did report, albeit minor, differences in the rhizosphere alpha and beta diversities by distance-based methods [22]. These contrasting results highlight a likely impact of plant age, soil type, environmental stimuli, and/or sampling on metabolite-microbiome interactions. Moreover, the difference in the impact of benzoxazinoids and diterpenoids on the rhizosphere diversity and community composition point toward distinct functionalities of different metabolite classes in maize-microbiome interactions. Recent analysis of two rice mutants, *Oscps2* and *Oscps4*, deficient in species-specific diterpenoids showed indistinguishable rhizosphere microbiomes and found to be from their WT siblings, suggesting that maize diterpenoids are distinct in their ability to modify the rhizosphere microbiome [47].

The lack of changes in the metabolite profiles of WT and *Zman2* roots beyond the expected dolabralexin deficiency in *Zman2* are consistent with WT phenotype of *Zman2* mutant plants under healthy conditions (Fig. 9) [16], and underscores that the observed microbiome alterations are a result of dolabralexin and/or kauralexin bioactivity rather than other metabolic perturbations caused by the ZmAN2 loss of function. Notably, a recent study investigating the root metabolome and microbiome in maize mutants deficient in the biosynthesis of selected benzoxazinoid compounds found the opposite effect, where mutant plants displayed significant metabolic changes across many pathways, which were predicted to have global effects on the microbiome, rather than changes in a specific metabolite group alone [23]. These works underscore the importance of metabolite analysis to understand the broader metabolic implications of pathway mutations especially within complex, branching metabolite networks.

Conclusions

Using a defined pathway mutant, the present study supports a role of species-specific bioactive maize diterpenoids in shaping the rhizosphere microbiome diversity and composition. These findings expand our insight into diterpenoid functions in Poaceous crops beyond well-established anti-microbial and anti-feedant bioactivities. Such deeper knowledge of the mechanisms underlying natural plant-microbe interactions will be critical for ultimately enabling broader agricultural applications.

Methods

Root exudate analysis

Seeds of *Zman2* and its isogenic wild type sibling (both in the W22 background) were obtained from Dr. Eric Schmelz (UC San Diego). Seeds (n = 5 for each genotype) were planted and grown in potting soil in 1 gallon pots in a greenhouse and watered with nutrient water, containing calcium nitrate (0.6 g/L water), Growmore (0.3 g/L water), and magnesium sulfate (0.3 g/L water). After 38 days, plants were removed

from pots and the roots were gently washed so as not to cause tissue damage. The plants were then placed in 2.8 L Erlenmeyer flasks and suspended with tape such that only the roots were in the nutrient water. Flasks were wrapped in aluminum foil to prevent light stress to the roots and placed in a growth chamber (as detailed below). After 48 hours, plants were removed, and the nutrient water was filtered through a metal strainer to remove any possible tissue debris. Metabolites were extracted from the exudate water by adding 700 mL of ethyl acetate to 700 mL exudate water and leaving at 4˚C for 24 hours. The organic solvent layer was then separated and concentrated using a rotary evaporator for metabolite analysis. Nutrient water containing no plants was used as a control.

Plant growth conditions

Soil was collected at UC Davis a research field site (coordinates 38.531152, -121.783182) by collecting approximately 6 inches of top soil using bleached shovels and collecting the soil in sterile bags. The field site had grown maize for one year, and at the time of collection (November 19, 2016) was fallow and had the stover previously turned under after the summer harvest. The soil was then mixed in the sterile bags and distributed to 2.37 L pots that were sterilized using 3% bleach wash. Plants were grown in a growth chamber in the pots in order to control for all other environmental conditions. The growth chamber was set to a 16/8 hour day/night cycle, with a 26/22˚C day/night temperature cycle. Seeds of *Zman2* and WT plants were sterilized in 3% (v/v) bleach for one hour, then washed five times with deionized water, and planted approximately 3 cm deep in the pots with maize field soil. Pots were distributed in the growth chamber in a block design to mitigate location effects. Treatment (drought vs well-watered) of *Zman2* and WT plants was measured for six biological replicates each using bulk soil (no plants) as a control.

Pots were watered every other day with 175 mL of nutrient water (see contents in root secretion assay methods). After 35 days, half of the plants (or bulk soil) were subject to drought treatment. Here, plants were not watered for six consecutive days in which the well-watered plants continued the previous watering and drought plants were not watered. After 6 days of drought treatment, the drought plants were given 140 mL of nutrient water to ensure that the plants received sufficient drought that the microbiome could respond to the treatment, but that the plants did not die. On the tenth day of drought treatment, all samples were harvested.

Microbiome sample collection

Sample collection and processing was adapted from Edwards, et al. 2015 [7]. In brief, plants were carefully removed from the soil, and gently shaken until ~ 2 mm of soil adhering to the root remained. n = 5 (bulk soil well-watered, bulk soil drought, rhizosphere drought *Zman2*, rhizosphere drought WT) or n = 6 (endosphere well-watered WT, drought WT, well-watered *Zman2*, drought *Zman2*; rhizosphere well-watered WT, well-watered *Zman2*); one plant from the drought *Zman2* and drought WT sample types was removed from the rhizosphere sample groups due to inadequate PCR amplification (see details below). The roots were then transferred to a 50 mL falcon tube contained sterile phosphate buffer saline (PBS) and placed on ice. For analysis of the rhizosphere microbiome, roots were shaken using sterile forceps to remove the soil from the root surface and soil samples were stored at 4˚C until further processing the next

day. For analysis of the endosphere microbiome, the above root samples were placed into fresh PBS buffer in a new 50 mL falcon tube and sonicated three 3 times for 10 s each, followed by placing the roots in fresh PBS buffer again to remove any rhizoplane microbes. Using these roots, ~ 4 cm sections of the primary root (beginning 2 cm below the root-shoot junction) was cut, placed in a new tube, frozen in liquid N_2, and stored at -80˚C until further processing. Bulk soil samples from soil 2 cm below the surface were collected using a sterile scoop and stored in PBS buffer at 4˚C until sample processing the next day.

After collecting all root and soil samples, remaining soil from each pot was collected in a 50 mL falcon tube and weighed. After drying the soil samples for one week at 65˚C, the samples were weighed again to determine the volumetric water content (VWC) of each sample.

DNA Extraction

All DNA was extracted using the MoBio PowerSoil DNA extraction kit and eluted in 50 µL of DEPC-treated water. The rhizosphere samples were concentrated by pipetting 1 mL of the rhizosphere soil in PBS into a 2 mL tube and centrifuged for 30 s at 10,000 x g. The supernatant was discarded and the soil was used for DNA extraction. The endosphere samples were homogenized and ground in liquid N_2 for DNA extraction with the MoBio Powersoil DNA kit.

16S rRNA gene amplification, quantitation, and sequencing

The V4 region (515 to 806 bp of the 16S rRNA gene) of the 16S rRNA gene was amplified according to Edwards et al. 2018 [48]. In brief, PCR was performed using Qiagen HotStart HiFidelity polymerase with the following parameters for each mix: 6.25 µL water, 2.5 µL buffer, 1.25 µL of 10 µM forward primer, 1.25 µL of 10 µM reverse primer, 0.25 µL HotStart polymerase, and 1 µL of DNA. Specific primer pairs, containing unique 12 bp barcode adaptors on each end of the forward and reverse primers were used for each reaction. Samples without DNA were used as negative controls. A touchdown PCR program was used with the following parameters: 95 ˚C for 5 min; 7 cycles of 95 ˚C for 45 sec, 65 ˚C for 1 min decreasing at 2 ˚C per cycle, and 72 ˚C for 90 sec; 30 cycles of 95 ˚C for 45 sec, 50 ˚C for 30 sec, 72 ˚C for 90 sec; a final extension of 72 ˚C for 5 min; and samples were held at 4 ˚C. Only samples producing single amplicon bands as verified by agarose gel electrophoresis were considered for further analysis, resulting in the loss of one biological replicate from each of the wild type drought rhizosphere sample group and one from the *ZmAn2* drought rhizosphere sample group.

Amplicons were purified to remove primers using AmPure XP beads (Beckman Coulter). Here, beads were added to each PCR reaction, incubated at room temperature for 5 min, and placed on a magnet for 2 min to separate the beads. After removal of the supernatant, the beads were washed with 70% ethanol twice. The ethanol was then allowed to evaporate and the beads were resuspended in 50 µL water, mixed well, and placed again on a magnet to remove the supernatant containing the desired PCR products. DNA concentrations were measured using a Qubit, and pooled to reach samples of equimolar concentrations. The pooled samples were cleaned as described above, separated by agarose gel electrophoresis and the 400 bp amplicons were extracted using a NucleoSpin Gel and PCR Clean-up kit (Macherey-Nagel).

Libraries were made and sequencing was performed at the UC Davis Genome Center using 250 × 250 paired end, dual index Illumina MiSeq sequencing.

Sequence analysis

Sequences were analyzed as previously described by Edwards et al. 2014 [7]. In brief, sequences were demultiplexed based on individual barcodes using a custom R script, and assembled into single sequences using PandasEq. Sequences were then clustered into OTUs with the NINJA-OPS pipeline using 97% pairwise sequence identity referenced against the Greengenes 16S rRNA sequence database (version 13_8) [32].

In total, 1,802,959 high-quality sequences were obtained with a median read count of 31,204 per sample, and a range of 1,699 – 87,795 (All data is available in Sequence Read Archive, Sequence Read Archive repository, BioProject ID PRJNA600272 [https://www.ncbi.nlm.nih.gov/sra/PRJNA600272]). Using the QIIME pipeline, reads were clustered based on 97% sequence identity into operational taxonomic units (OTUs) and were annotated using QIIME and the Greengenes database [32], resulting in 7,181 microbial OTUs. Chloroplast and mitochondrial OTUs represented 65 OTUs and were removed, along with low-abundance OTUs (less than 5% of the total sample), leaving 4,258 total OTUs. OTU counts were then normalized by relative abundance, which was used rather than rarefaction methods so as not to discard low abundance OTUs.

All statistical analysis of the OTU table generated by QIIME [32] were analyzed using custom R scripts (version 3.6.1) [49]. Alpha-diversity was measured using the “Shannon” method in the R package vegan [50]. Principle coordinate analysis (PCoA) were conducted using unconstrained principles and Bray distances in the R package vegan [50]. PERMANOVA (permutational multivariate analyses of variance) analysis was performed using the R package vegan function adonis to measure beta-diversity [50]. The DESeq2 package [51] was used to analyze differentially abundant phyla, that were collapsed OTU counts, and individual OTUs, along with the biobroom package [52]. Plots were visualized using the ggplot2 in the tidyverse package [53]. All scripts generated in this study have been deposited to GitHub (https://github.com/kmurphy61/maizemicrobiome).

Metabolite extraction

The remaining roots (~ 1 g fresh weight) used for endosphere microbiome analysis (see microbiome sample collection) were homogenized and ground in liquid nitrogen. Because of availability of tissue, the number of plant samples were reduced for metabolite extraction as compared to microbiome DNA extraction; n = 4 (WT well-watered, *Zman2* well-watered, *Zman2* drought) or n = 3 (WT drought). Samples were then placed in a 2 mL glass vial and metabolites extracted by incubation in 2 mL methanol overnight at 4°C with gentle rocking. Samples were centrifuged for 10 min at 4000 x g and the methanol phase transferred to a new vial using a glass pipette, air-dried, and resuspended in either 100 or 200 µL methanol.

Metabolite analysis

For metabolite analysis by liquid chromatography tandem mass spectrometry (LC-MS/MS), samples were spiked with 4 µM internal standard mixture of deuterium-labeled lipids (Cat# 110899, 857463P, 861809O, 110922, 110922, 110921, 110918, 110579, 110544, Avanti Polar Lipids, Inc) and 1 µg/mL ABMBA (2-Amino-3-bromo-5-methylbenzoic acid, Sigma). UHPLC reverse phase chromatography was performed using an Agilent 1290 LC coupled with a QExactive Orbitrap MS (QE = 139) (Thermo Scientific, San Jose, CA). Chromatography was performed using a C18 column (Agilent ZORBAX Eclipse Plus C18, Rapid Resolution HD, 2.1 × 50 mm, 1.8 µm) at a flow rate of 0.4 mL/min and injection volume varied from 0.9 to 3.5 µL to normalize against sample dry weight. Samples were run on the C18 column at 60 ºC equilibrated with 100% buffer A (100% LC-MS water w/ 0.1% formic acid) for 1 min, following by a linear dilution of buffer A down to 0% with buffer B (100% acetonitrile w/ 0.1% formic acid) over 7 min, and followed by isocratic elution in 100% buffer B for 1.5 min. Full MS spectra were collected ranging from *m/z* 80 – 2,000 at 60,000 to 70,000 resolution in both positive and negative mode, with MS/MS fragmentation data acquisition using an average of stepped 10-20-40 and 20-50-60 eV collision energies at 17,500 resolution. For targeted analysis, product identification by comparison to standards was performed where authentic standards were available.

For untargeted analysis, exact mass and retention time coupled with MS/MS fragmentation spectra were used to identify compounds. Features - high intensity signals narrowly contained at a given retention time and *m/z* - were detected using the MZMine software v 2.24 (http://dx.doi.org/10.1093/bioinformatics/btk039). Further custom Python scripts were used to identify minimum and maximum retention time bounds for each peak, filter peaks that were not at least 3 times higher in a sample compared to all injection blanks, and filter peaks that did not have at least one MS/MS spectrum. Complete feature lists are available on GitHub (https://github.com/kmurphy61/maizemicrobiome.git). Features that showed a significantly different abundance (peak area) using linear models, calculated using custom R scripts[49]. Significantly different features were annotated using custom Python scripts. A wide range of chemical standards previously added to a mass spectral library were used to annotate metabolite identifications based on matching *m/z* better than 10 parts per million (ppm), retention time better than 0.1 minutes, and matching fragmentation patterns better than a score of 0.7. The remaining compounds that met these criteria were added to a Metabolite Atlas (http://dx.doi.org/10.3390/metabo5030431) for positive and negative ionization modes. All scripts are available on GitHub (https://github.com/kmurphy61/maizemicrobiome.git). Additionally, enriched features were analyzed using PACTOLUS (https://github.com/biorack/pactolus). Significantly different features by sample type are available in Supplemental Tables 1 (well-watered), 2 (drought), 3 (WT), and 4 (*Zman2*).

List Of Abbreviations

OTU, operational taxonomic unit; GGDP, geranylgeranyl diphosphate; CDP, copalyl diphosphate; diTPS, diterpenoid synthase; P450, cytochrome P450 monooxygenase; LC/MS, liquid chromatography, mass spectrometry; GA, gibberellin

Declarations

Ethics Approval and Consent to Participate

Not Applicable

Consent for Publication

Not Applicable

Availability of Data and Material

The datasets generated during and/or analyzed during this study are available in the Sequence Read Archive repository, BioProject ID PRJNA600272 [https://www.ncbi.nlm.nih.gov/sra/PRJNA600272]. The code used to analyze these datasets are available in the GitHub repository, https://github.com/kmurphy61/maizemicrobiome.git.

Competing Interests.

The authors declare that they have no conflict of interest in accordance with the journal policy.

Funding
Financial support for this work was provided by the National Science Foundation (NSF) Plant-Biotic Interactions Program (Award# 1758976 to PZ), the NSF Graduate Research Fellowship Program (to KMM), the UC Davis Innovation Institute for Food and Health (IIFH) Fellowship Program (to KMM & PZ), and the USDA NIFA Predoctoral Fellowship Program (Award# 2019-67011-29544 to KMM). The work conducted by the US Department of Energy Joint Genome Institute, a DOE Office of Science User Facility, is supported under contract no. DE-AC02-05CH11231. This manuscript has been authored by an author at Lawrence Berkeley National Laboratory under Contract No. DE-AC02-05CH11231 with the U.S. Department of Energy. The U.S. Government retains, and the publisher, by accepting the article for publication, acknowledges, that the U.S. Government retains a non-exclusive, paid-up, irrevocable, world-wide license to publish or reproduce the published form of this manuscript, or allow others to do so, for U.S. Government purposes.

Authors contributions.

KMM and PZ designed the experiments; TRN advised on metabolomics experiments; KMM performed most experiments; KMM and JE performed microbiome analyses; KBL and BPB performed LC/MS experiments and data analysis; KMM and PZ wrote the article with contributions of all other authors.

Acknowledgements
The authors gratefully acknowledge Dr. Eric Schmelz (UC San Diego), for providing seeds of *Zman2* and WT plants used in this study. They also acknowledge Zach Liechty (UC Davis) and Christian Santos-Medellín (UC Davis) for their advising in data analysis and computation.

References

1. Korenblum E, Aharoni A. Phytobiome metabolism: beneficial soil microbes steer crop plants' secondary metabolism. Pest Manag Sci. 2019;75(9):2378–84. doi:.
2. Mitter B, Brader G, Pfaffenbichler N, Sessitsch A. Next generation microbiome applications for crop production - limitations and the need of knowledge-based solutions. Curr Opin Microbiol. 2019;49:59–65. doi:.
3. Xu L, Coleman-Derr D. Causes and consequences of a conserved bacterial root microbiome response to drought stress. Curr Opin Microbiol. 2019;49:1–6. doi:.
4. Berendsen RL, Pieterse CM, Bakker PA. The rhizosphere microbiome and plant health. Trends Plant Sci. 2012;17(8):478–86. doi:.
5. Castrillo G, Teixeira PJPL, Paredes SH, Law TF, de Lorenzo L, Feltcher ME, et al. Root microbiota drive direct integration of phosphate stress and immunity. Nature. 2017;543(7646):513-+. doi:.
6. Niu B, Paulson JN, Zheng XQ, Kolter R. Simplified and representative bacterial community of maize roots. P Natl Acad Sci USA. 2017;114(12):E2450-E9. doi:.
7. Edwards J, Johnson C, Santos-Medellin C, Lurie E, Podishetty NK, Bhatnagar S, et al. Structure, variation, and assembly of the root-associated microbiomes of rice. Proc Natl Acad Sci U S A. 2015;112(8):E911-20. doi:.
8. Aira M, Gomez-Brandon M, Lazcano C, Baath E, Dominguez J. Plant genotype strongly modifies the structure and growth of maize rhizosphere microbial communities. Soil Biol Biochem. 2010;42(12):2276–81. doi:.
9. Garcia-Salamanca A, Molina-Henares MA, van Dillewijn P, Solano J, Pizarro-Tobias P, Roca A, et al. Bacterial diversity in the rhizosphere of maize and the surrounding carbonate-rich bulk soil. Microb Biotechnol. 2013;6(1):36–44. doi:.
10. de Oliveira CA, Marriel IE, Gomes EA, Lana UGD, Scotti MR, Alves VMC. Bacterial diversity in the rhizosphere of maize genotypes contrasting for phosphorus use efficiency. Pesqui Agropecu Bras. 2009;44(11):1473–82.
11. Haichar FE, Marol C, Berge O, Rangel-Castro JI, Prosser JI, Balesdent J, et al. Plant host habitat and root exudates shape soil bacterial community structure. Isme J. 2008;2(12):1221–30. doi:.
12. Savary S, Willocquet L, Pethybridge SJ, Esker P, McRoberts N, Nelson A. The global burden of pathogens and pests on major food crops. Nature Ecology Evolution. 2019;3(3):430-+. doi:.
13. Lundberg DS, Lebeis SL, Paredes SH, Yourstone S, Gehring J, Malfatti S, et al. Defining the core Arabidopsis thaliana root microbiome. Nature. 2012;488(7409):86-+. doi:.
14. Walters WA, Jin Z, Youngblut N, Wallace JG, Sutter J, Zhang W, et al. Large-scale replicated field study of maize rhizosphere identifies heritable microbes. Proc Natl Acad Sci U S A. 2018. doi:.
15. Christensen SA, Huffaker A, Kaplan F, Sims J, Ziemann S, Doehlemann G, et al. Maize death acids, 9-lipoxygenase-derived cyclopente(a)nones, display activity as cytotoxic phytoalexins and transcriptional mediators. Proc Natl Acad Sci U S A. 2015;112(36):11407–12. doi:.

16. Vaughan MM, Christensen S, Schmelz EA, Huffaker A, McAuslane HJ, Alborn HT, et al. Accumulation of terpenoid phytoalexins in maize roots is associated with drought tolerance. Plant Cell Environ. 2015;38(11):2195–207. doi:.
17. Schmelz EA, Kaplan F, Huffaker A, Dafoe NJ, Vaughan MM, Ni X, et al. Identity, regulation, and activity of inducible diterpenoid phytoalexins in maize. Proc Natl Acad Sci U S A. 2011;108(13):5455–60. doi:.
18. Mafu S, Ding Y, Murphy KM, Yaacoobi O, Addison JB, Wang Q, et al. Discovery, biosynthesis and stress-related accumulation of dolabradiene-derived defenses in maize. Plant Physiol. 2018. doi:.
19. Huffaker A, Kaplan F, Vaughan MM, Dafoe NJ, Ni X, Rocca JR, et al. Novel acidic sesquiterpenoids constitute a dominant class of pathogen-induced phytoalexins in maize. Plant Physiol. 2011;156(4):2082–97. doi:.
20. Ahmad S, Veyrat N, Gordon-Weeks R, Zhang Y, Martin J, Smart L, et al. Benzoxazinoid metabolites regulate innate immunity against aphids and fungi in maize. Plant Physiol. 2011;157(1):317–27. doi:.
21. Hu L, Robert CAM, Cadot S, Zhang X, Ye M, Li B, et al. Root exudate metabolites drive plant-soil feedbacks on growth and defense by shaping the rhizosphere microbiota. Nat Commun. 2018;9(1):2738. doi:.
22. Kudjordjie EN, Sapkota R, Steffensen SK, Fomsgaard IS, Nicolaisen M. Maize synthesized benzoxazinoids affect the host associated microbiome. Microbiome. 2019;7(1):59. doi:.
23. Cotton TEA, Petriacq P, Cameron DD, Meselmani MA, Schwarzenbacher R, Rolfe SA, et al. Metabolic regulation of the maize rhizobiome by benzoxazinoids. ISME J. 2019. doi:.
24. Huang AC, Osbourn A. Plant terpenes that mediate below-ground interactions: prospects for bioengineering terpenoids for plant protection. Pest Manag Sci. 2019;75(9):2368–77. doi:.
25. Block AK, Vaughan MM, Schmelz EA, Christensen SA. Biosynthesis and function of terpenoid defense compounds in maize (Zea mays). Planta. 2019;249(1):21–30. doi:.
26. Christensen SA, Sims J, Vaughan MM, Hunter C, Block A, Willett D, et al. Commercial hybrids and mutant genotypes reveal complex protective roles for inducible terpenoid defenses in maize. J Exp Bot. 2018;69(7):1693–705. doi:.
27. Christie N, Myburg AA, Joubert F, Murray SL, Carstens M, Lin YC, et al. Systems genetics reveals a transcriptional network associated with susceptibility in the maize-grey leaf spot pathosystem. Plant J. 2017;89(4):746–63. doi:.
28. Schmelz EA, Huffaker A, Sims JW, Christensen SA, Lu X, Okada K, et al. Biosynthesis, elicitation and roles of monocot terpenoid phytoalexins. Plant J. 2014;79(4):659–78. doi:.
29. Harris LJ, Saparno A, Johnston A, Prisic S, Xu M, Allard S, et al. The maize An2 gene is induced by Fusarium attack and encodes an ent-copalyl diphosphate synthase. Plant Mol Biol. 2005;59(6):881–94. doi:.
30. Bensen RJ, Johal GS, Crane VC, Tossberg JT, Schnable PS, Meeley RB, et al. Cloning and characterization of the maize An1 gene. Plant Cell. 1995;7(1):75–84. doi:.

31. Ding Y, Murphy KM, Poretsky E, Mafu S, Yang B, Char SN, et al. Multiple genes recruited from hormone pathways partition maize diterpenoid defences. Nat Plants. 2019;5(10):1043–56. doi:.
32. Caporaso JG, Kuczynski J, Stombaugh J, Bittinger K, Bushman FD, Costello EK, et al. QIIME allows analysis of high-throughput community sequencing data. Nat Methods. 2010;7(5):335–6. doi:.
33. Naylor D, DeGraaf S, Purdom E, Coleman-Derr D. Drought and host selection influence bacterial community dynamics in the grass root microbiome. ISME J. 2017;11(12):2691–704. doi:.
34. Naylor D, Coleman-Derr D. Drought Stress and Root-Associated Bacterial Communities. Front Plant Sci. 2017;8:2223. doi:.
35. Santos-Medellín C, Edwards J, Liechty Z, Nguyen B, Sundaresan V. Drought Stress Results in a Compartment-Specific Restructuring of the Rice Root-Associated Microbiomes. MBio. 2017;8(4); doi:.
36. James EK, Gyaneshwar P, Mathan N, Barraquio WL, Reddy PM, Iannetta PP, et al. Infection and colonization of rice seedlings by the plant growth-promoting bacterium Herbaspirillum seropedicae Z67. Mol Plant Microbe Interact. 2002;15(9):894–906. doi:.
37. Turner TR, James EK, Poole PS. The plant microbiome. Genome Biol. 2013;14(6):209. doi:.
38. Liu H, Carvalhais LC, Crawford M, Singh E, Dennis PG, Pieterse CMJ, et al. Inner Plant Values: Diversity, Colonization and Benefits from Endophytic Bacteria. Front Microbiol. 2017;8:2552. doi:.
39. Lange BM, Fischedick JT, Lange MF, Srividya N, Šamec D, Poirier BC. Integrative Approaches for the Identification and Localization of Specialized Metabolites in Tripterygium Roots. Plant Physiol. 2017;173(1):456–69. doi:.
40. Pateraki I, Andersen-Ranberg J, Hamberger B, Heskes AM, Martens HJ, Zerbe P, et al. Manoyl oxide (13R), the biosynthetic precursor of forskolin, is synthesized in specialized root cork cells in Coleus forskohlii. Plant Physiol. 2014;164(3):1222–36. doi:.
41. Vaughan MM, Wang Q, Webster FX, Kiemle D, Hong YJ, Tantillo DJ, et al. Formation of the unusual semivolatile diterpene rhizathalene by the Arabidopsis class I terpene synthase TPS08 in the root stele is involved in defense against belowground herbivory. Plant Cell. 2013;25(3):1108–25. doi:.
42. Kim SJ, Chun J, Bae KS, Kim YC. Polyphasic assignment of an aromatic-degrading Pseudomonas sp., strain DJ77, in the genus Sphingomonas as Sphingomonas chungbukensis sp. nov. Int J Syst Evol Microbiol. 2000;50(Pt 4):1641–7. doi:.
43. van Elsas JD, Chiurazzi M, Mallon CA, Elhottova D, Kristufek V, Salles JF. Microbial diversity determines the invasion of soil by a bacterial pathogen. Proc Natl Acad Sci U S A. 2012;109(4):1159–64. doi:.
44. Wei Z, Yang TJ, Friman VP, Xu YC, Shen QR, Jousset A. Trophic network architecture of root-associated bacterial communities determines pathogen invasion and plant health. Nature Communications. 2015;6; doi: ARTN 8413.
45. 1038/ncomms9413.
46. Vaughan MM, Huffaker A, Schmelz EA, Dafoe NJ, Christensen S, Sims J, et al. Effects of elevated [CO2] on maize defence against mycotoxigenic Fusarium verticillioides. Plant Cell Environ.

2014;37(12):2691–706. doi:.
47. Cotton TEA, Pétriacq P, Cameron DD, Meselmani MA, Schwarzenbacher R, Rolfe SA, et al. Metabolic regulation of the maize rhizobiome by benzoxazinoids. ISME J. 2019;13(7):1647–58. doi:.
48. Lu X, Zhang J, Brown B, Li R, Rodriguez-Romero J, Berasategui A, et al. Inferring Roles in Defense from Metabolic Allocation of Rice Diterpenoids. Plant Cell. 2018. doi:.
49. Edwards J, Santos-Medellín C, Sundaresan V. Extraction and 16S rRNA Sequence Analysis of Microbiomes Associated with Rice Roots. 2018;8(12): e2884; doi: .
50. Team RC. R: A language and environment for statistical computing. R Foundation for Statistical Computing. (2019). Accessed.
51. Oksanen J, Blanchet FG, Friendly M, Kindt R, Legendre P, McGlinn D, et al. vegan: Community Ecology Package. R package version 2.5-6. (2019). Accessed.
52. Love MI, Huber W, Anders S. Moderated estimation of fold change and dispersion for RNA-seq data with DESeq2. Genome Biol. 2014;15(12):550. doi:.
53. Bass AJ, Robinson DG, Lianoglou S, Nelson E, Storey JD, Gatto L. biobroom. Turn Bioconductor objects into tidy data frames. R package version 1.16.0. (2019). Accessed.
54. Wickham H. tidyverse: Easily Install and Load the 'Tidyverse'. R package version 1.2.1. (2017). Accessed.

Figures

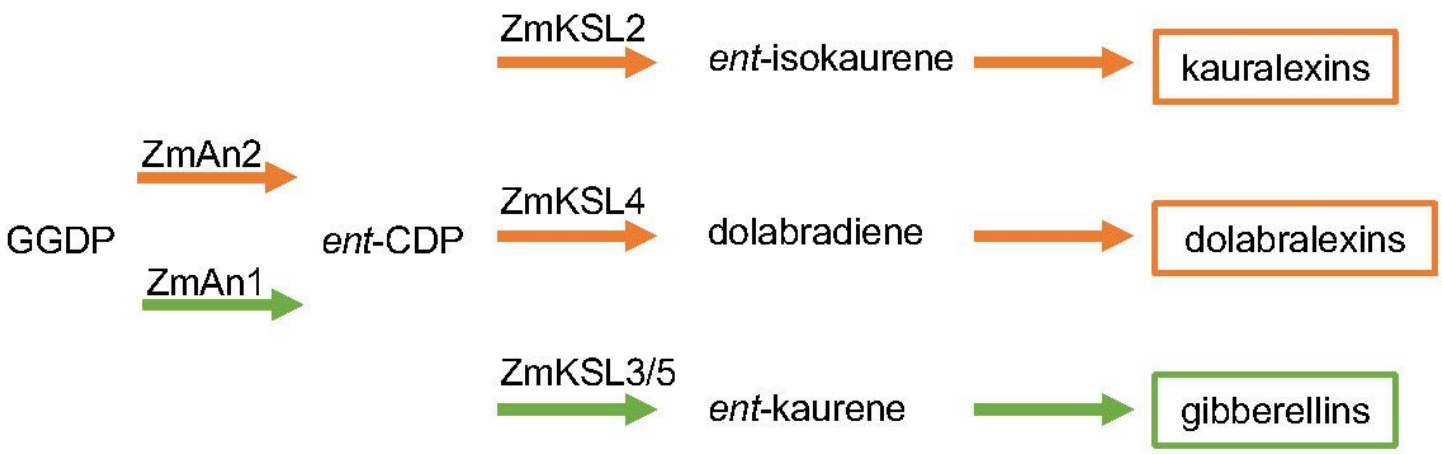

Figure 1

Schematic overview of key enzymes involved in diterpenoid biosynthesis in maize. Abbreviations: GGDP, (E,E,E)-geranyl geranyl diphosphate; ent-CDP, copalyl diphosphate; An, anther ear; KSL, kaurene synthase-like. Orange arrows represent pathways en route to specialized, defensive metabolites. Green pathways represent gibberellin hormone biosynthesis.

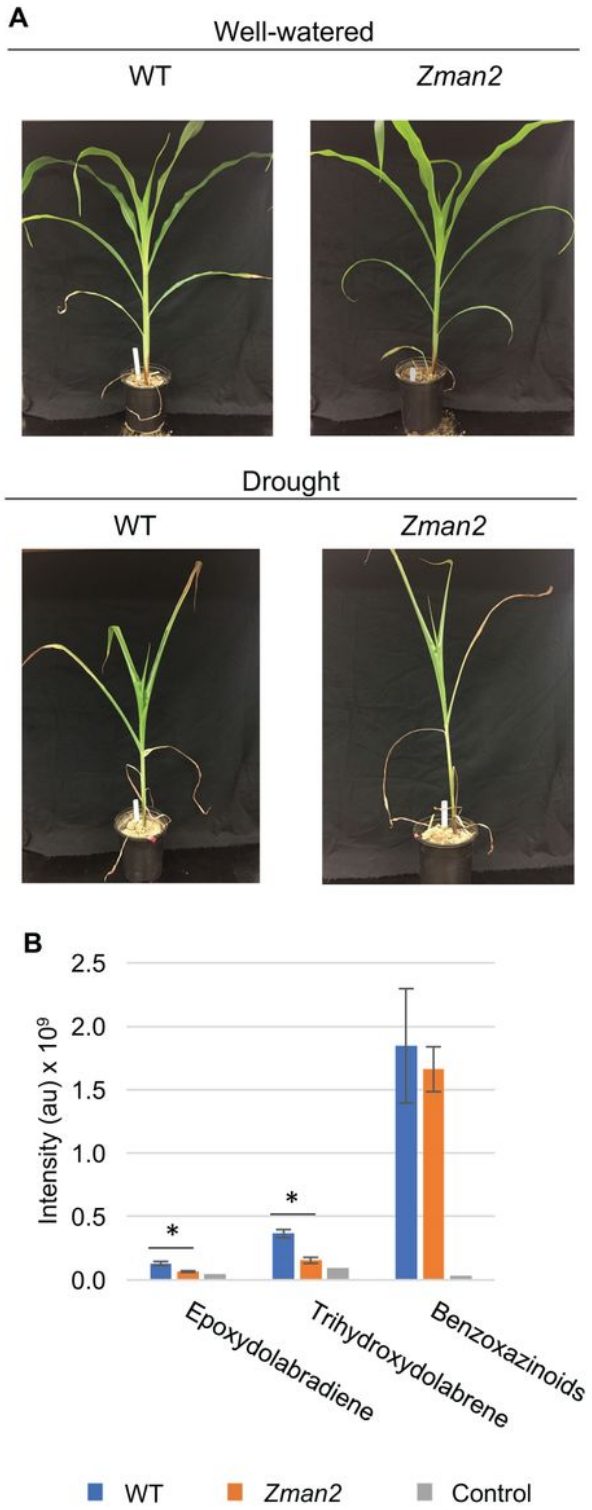

Figure 2

Phenotype and metabolite abundance in maize Zman2 mutants and WT plants. (A) Representative images of Zman2 mutant plants and the corresponding WT sibling used in this study under well-watered and drought conditions. (B) Average intensity of metabolites in maize root exudate samples using positive mode LC-MS/MS analysis. Peak area given for epoxydolabradiene [M+H], trihydroxydolabrene [M+H-H2O], and benzoxazinoids, with the last based on detection of metabolites containing BOA (1,3-

benzoxazol-2-one (BOA) [M+H]). * represents significant difference between two sample types, $p \leq 0.05$. Two-tailed t-tests were used for benzoxazinoids; one-tailed t-tests were used for dolabralexins, since they are predicted to be enriched in WT and deficient in Zman2. Error bars represent standard error. n = 5 (WT, Zman2); Control represents one extraction of nutrient water, and demonstrates LC-MS/MS background.

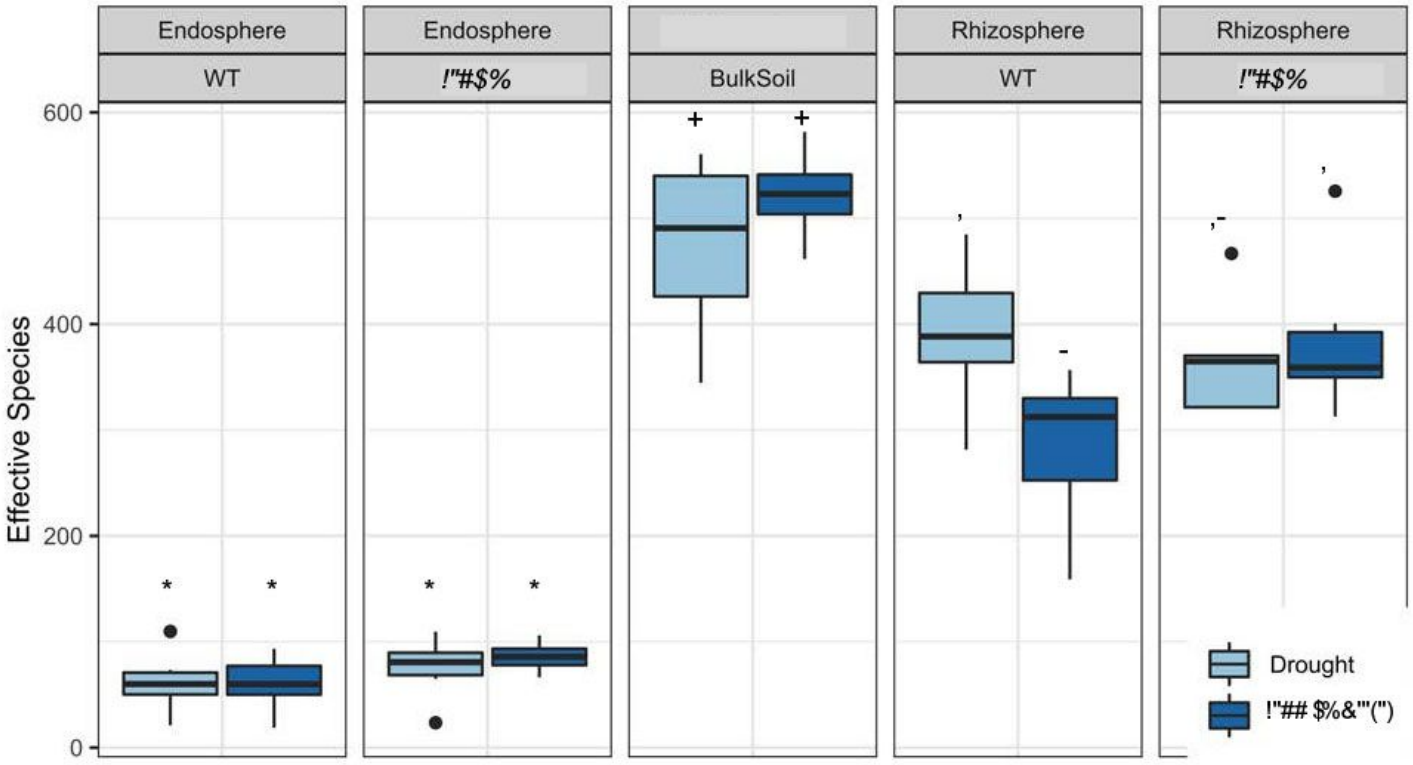

Figure 3

Alpha diversity of each sample type, as measured by the Shannon's H index. Letters represent significantly different measurements determined using PERMANOVA, $p \leq 0.05$. n= 5 (bulk soil well-watered, bulk soil drought, rhizosphere drought Zman2, rhizosphere drought WT) or n = 6 (endosphere well-watered WT, drought WT, well-watered Zman2, drought Zman2; rhizosphere well-watered WT, well-watered Zman2).

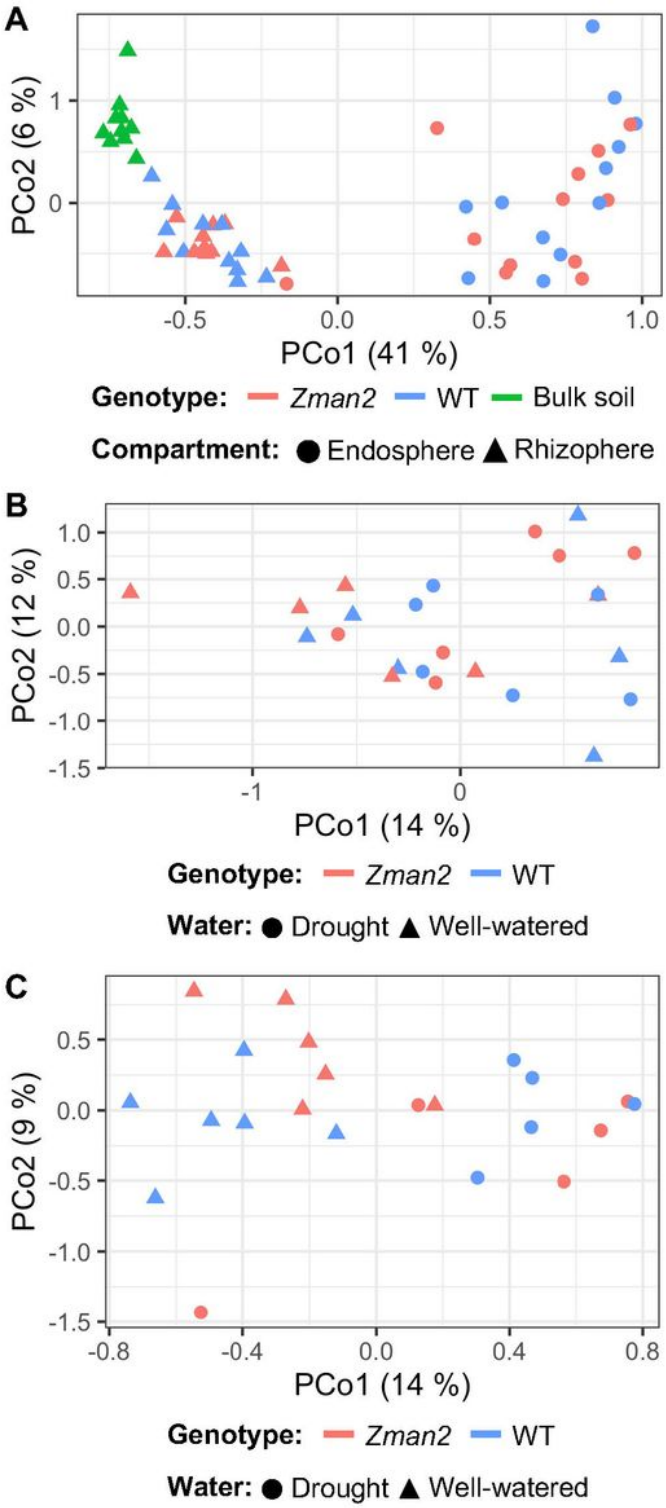

Figure 4

Principal Coordinate Analysis (PCoA) using wunifraq distances for (A) all samples, (B) endosphere only, and (C) the rhizosphere only. Each point represents an individual plant or soil sample. Percentage in the axis labels represents the eigenvalue, or percent of variation explained by that axis

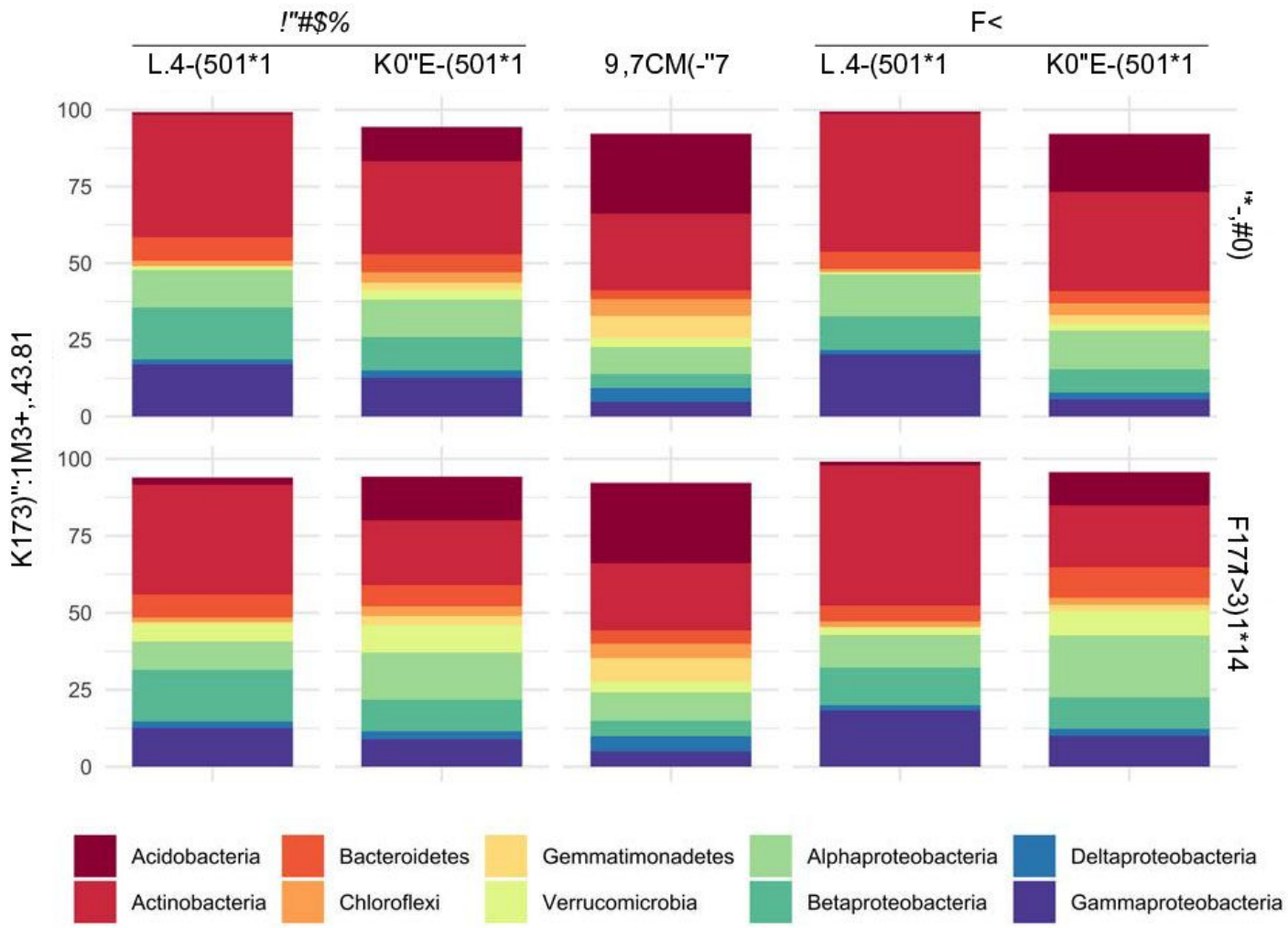

Figure 5

Distribution of the ten most abundant phyla for each sample type. Bars represent the relative abundance of all OTUs within each of the top 10 most abundant phyla. n= 5 (bulk soil well watered, bulk soil drought, rhizosphere drought Zman2, rhizosphere drought WT) or n = 6 (endosphere well-watered WT, drought WT, well-watered Zman2, drought Zman2; rhizosphere well-watered WT, well-watered Zman2).

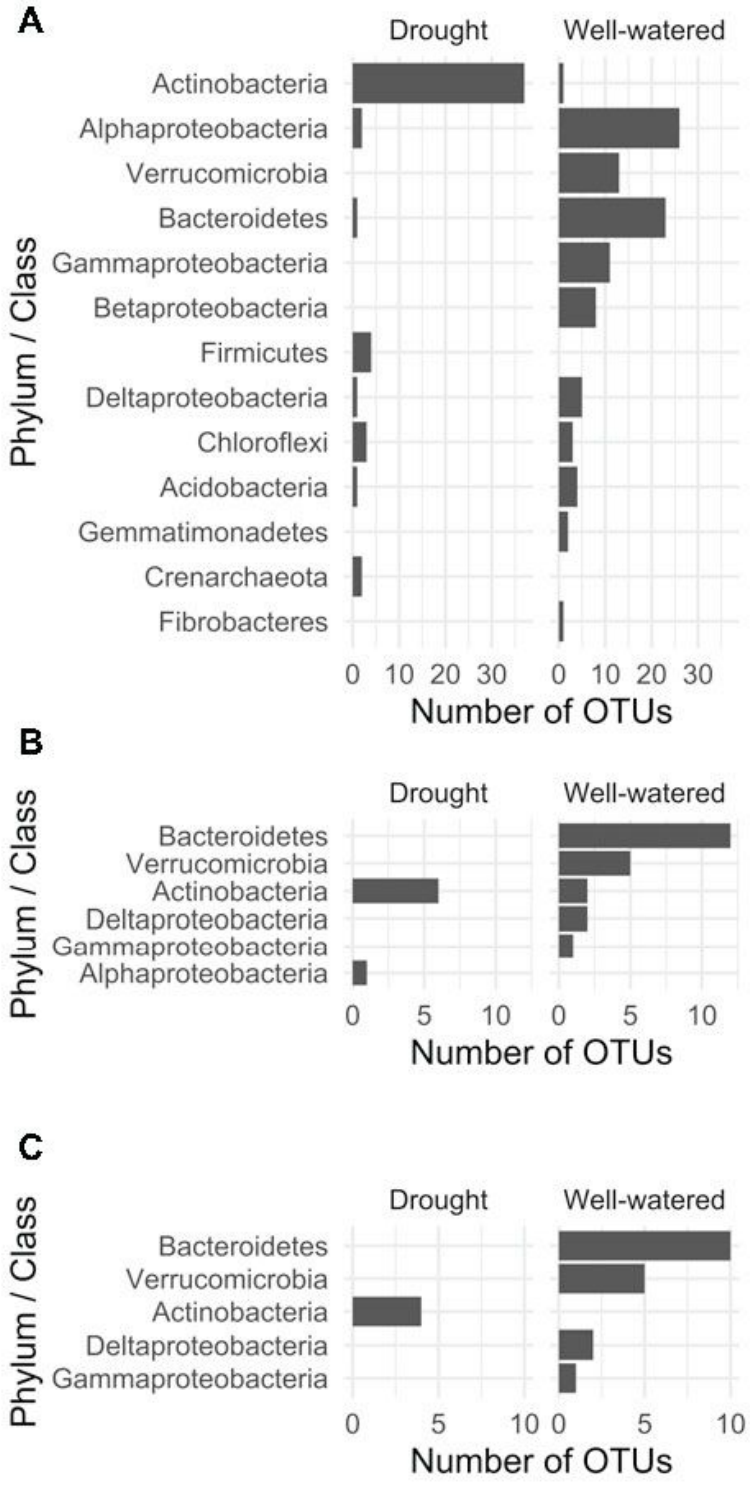

Figure 6

Significantly different OTUs detected using linear methods and their respective Phyla in the (A) rhizosphere, (B) bulk soil control, or (C) both the rhizosphere and bulk soil control, irrespective of genotype. n = 5 (bulk soil well-watered, bulk soil drought) or n = 11 (rhizosphere well-watered, rhizosphere drought).

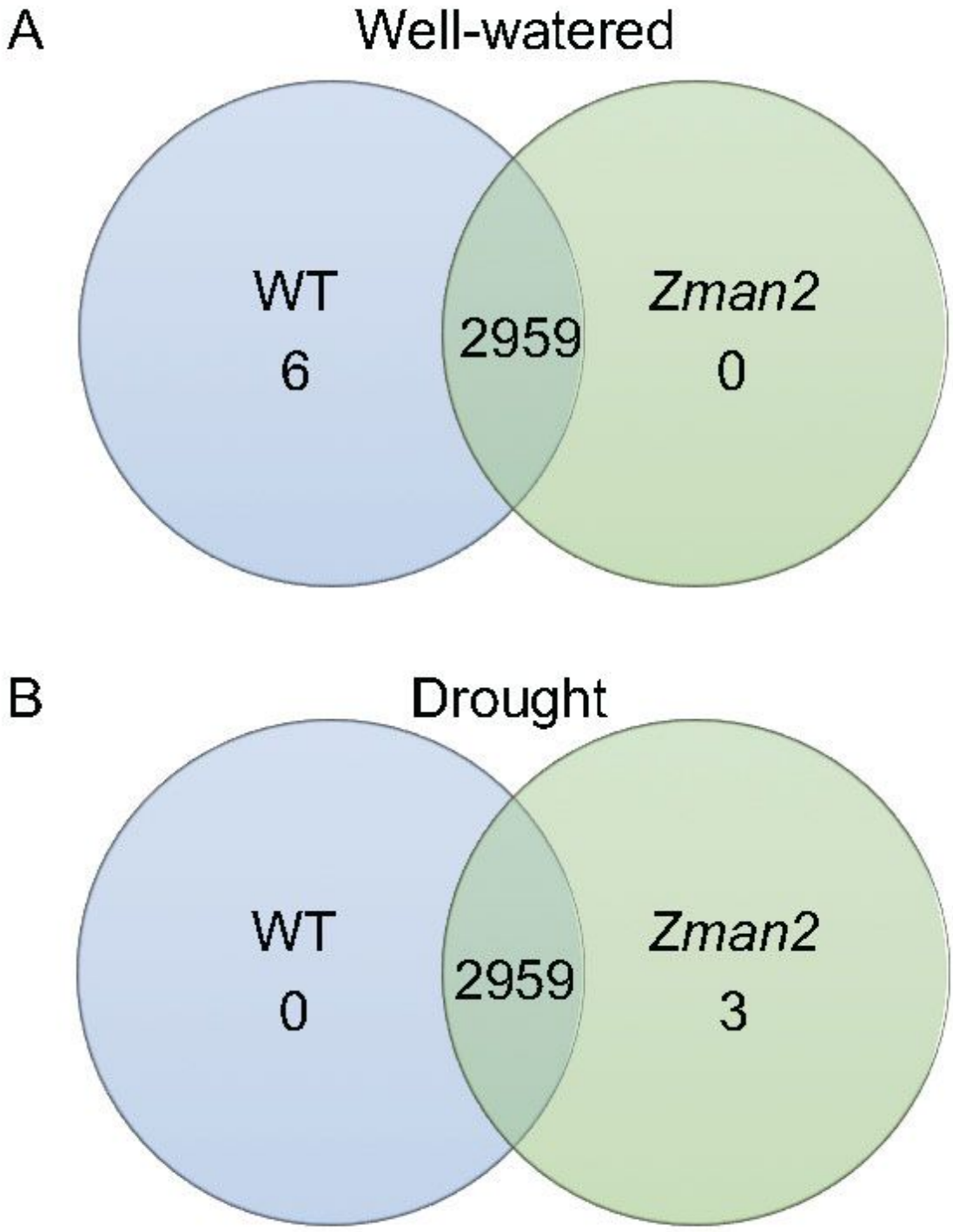

Figure 7

Differentially expressed OTUs in the rhizosphere, as measured by a linear model for genotype in (A) well-watered or (B) drought conditions. Overlap is non-significantly different OTUs, at the level of $p \leq 0.05$. n = 6 (well-watered) or n = 5 (drought) per genotype.

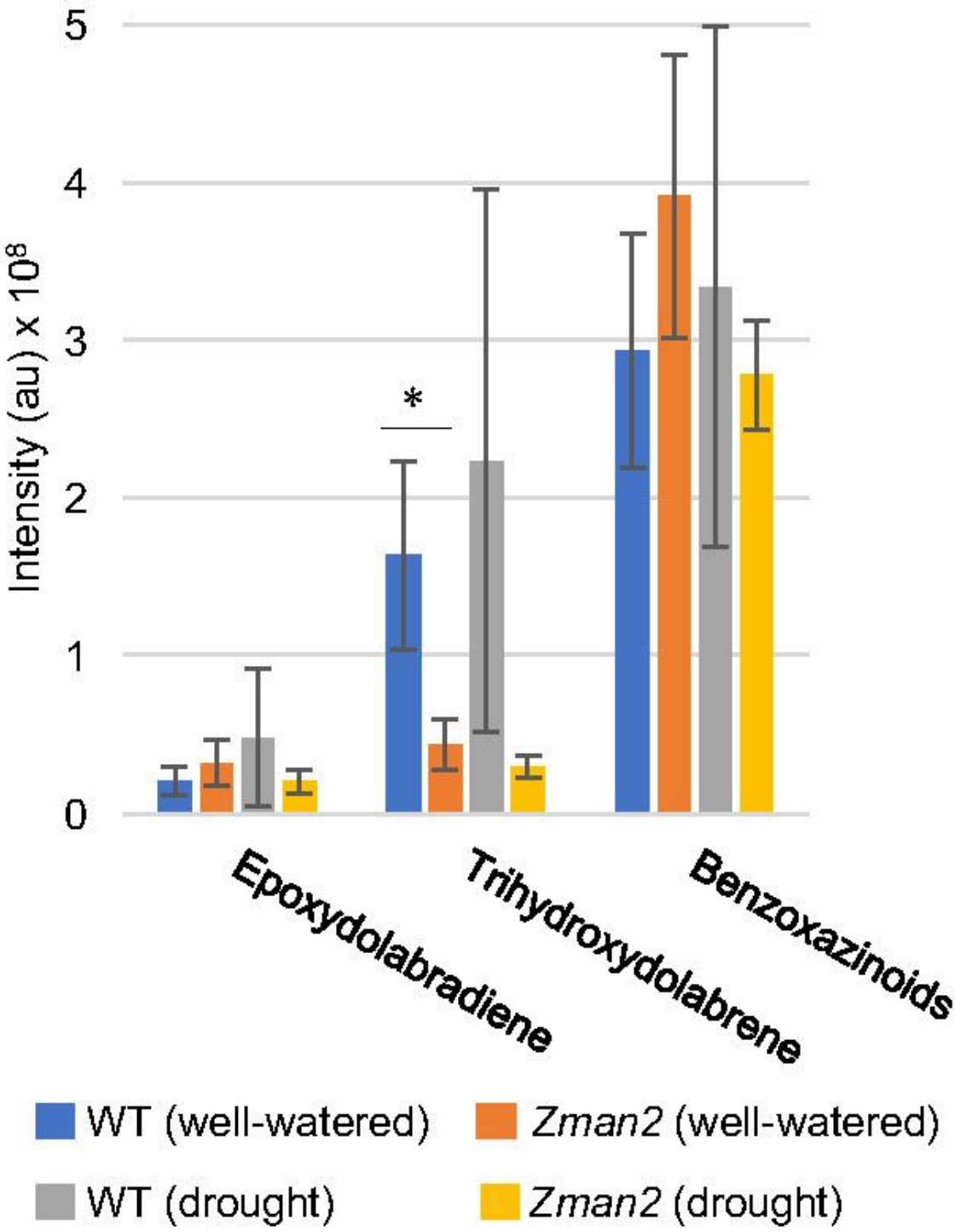

Figure 8

Average intensity of metabolites in maize root samples using positive mode LC-MS/MS peak area. Peak area based on epoxydolabradiene [M+H], trihydroxydolabrene [M+H-H2O], and benzoxazinoids, with the last based on detection of metabolites containing BOA (1,3-benzoxazol-2-one (BOA) [M+H]). * represents significant difference between two samples $p \leq 0.05$. Two-tailed t-tests were used for benzoxazinoids; one-tailed t-tests were used for the remaining metabolites, since they are predicted to be enriched in WT

and deficient in Zman2. n = 4 (WT well-watered, Zman2 well-watered, Zman2 drought) or n = 3 (WT drought). Error bars represent standard error.

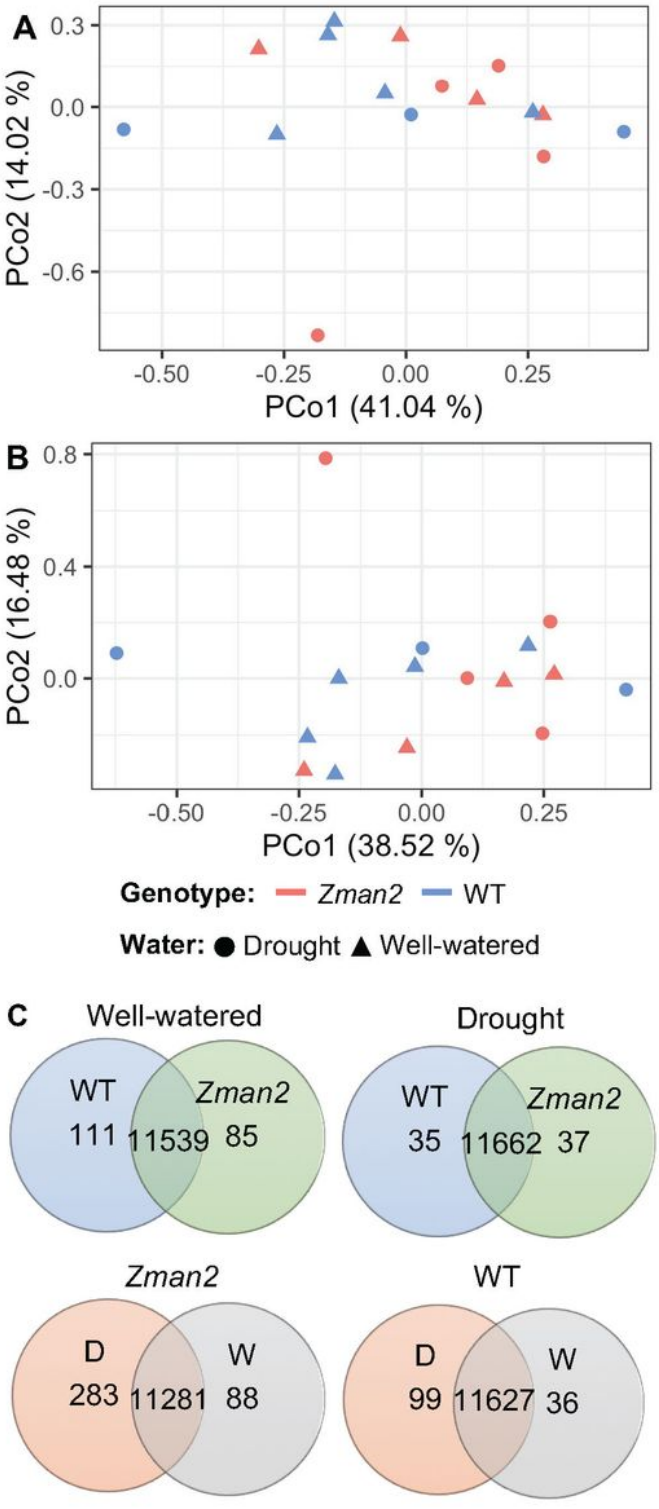

Figure 9

Principal Coordinate Analysis (PCoA) of the metabolome for all root samples in (A) positive mode or (B) negative mode using LC-MS/MS. n = 4 (WT well-watered, Zman2 well-watered, Zman2 drought) or n = 3 (WT drought). Each point represents an individual plant sample. Percentage in the axis labels represents

the eigenvalue, or percent of variation explained by that axis. (C) Number of enriched metabolites detected using LC-MS/MS in positive mode, as measured by a linear model at the level of $p \leq 0.05$, for each sample type. Overlap are not significantly different. n = 4 (WT well-watered, Zman2 well-watered, Zman2 drought) or n = 3 (WT drought).

Supplementary Files

This is a list of supplementary files associated with this preprint. Click to download.

- SuppTable3.xlsx
- MurphyetalSuppFig1.pdf
- MurphyetalSuppFig3.pdf
- MurphyetalSuppFig2.pdf
- MurphyetalSuppFig4.pdf
- SuppTable2.xlsx
- MurphyetalSuppFig5.pdf
- SuppTable1.xlsx
- SuppTable4.xlsx